

# XRD, Raman and SEM surface analysis on Ni-Cu electrodeposited layers

O.-C. CIOBOTEA-BARBU<sup>a,b</sup>, I.-A. CIOBOTARU<sup>a</sup>, D.-I. VAIREANU<sup>a,\*</sup>, D. G. DUMITRAS<sup>b</sup>, C. NICOLAE<sup>b</sup>

<sup>a</sup>University POLITEHNICA of Bucharest, Faculty of Applied Chemistry and Materials Science, 1-7 Polizu Street, 011061, Bucharest, Romania

<sup>b</sup>Geological Institute of Romania, 1 Caransebes Street, 01227, Bucharest, Romania

This paper presents the characterization of a Ni-Cu thin layer electrodeposited onto a steel substrate. The characterization of these films was performed with X-ray diffraction spectroscopy, Raman spectroscopy and Scanning electron microscopy. The results of the XRD analysis showed a Face Centered Cubic structure and the Raman spectroscopy indicated the presence of Cu<sub>2</sub>O, CuO and NiO into the films.

(Received October 18, 2018; accepted August 20, 2019)

**Keywords:** Electrodeposited Ni-Cu films, surface analysis, XRD, Raman, SEM

## 1. Introduction

Thin deposited metallic films such as Fe, Ni, Co, Cu have attracted a lot of interest for a long time due to their inherent potential applications in data storage devices [1], nanostructural designed materials, corrosion protective coatings and their electronic properties [2].

Electrodeposition is one of the most employed techniques used to obtain nanocrystalline metallic films, with thicknesses ranging from hundreds of nanometers to tens of micrometers [3].

Surface science is a subject that grew enormously in the last decade, partly because of the availability of some new electron-based tools. X-ray diffraction spectroscopy and Raman spectroscopy, techniques also used in the present study, have contributed to many advances in the field [4-7].

The aim of this study is to characterize some Ni-Cu films electrodeposited on steel substrates. The morphological properties of these films were evaluated by means of scanning electron microscopy. X-ray diffraction spectroscopy and Raman spectroscopy were employed in order to determine the crystallization system of the Ni-Cu alloys, respectively to determine the presence of Ni and Cu in the deposits. These methods were employed for the determination of the structural and morphological properties of the Ni-Cu alloys, because one needed a confirmation of the presence of copper and nickel in the composition of the final alloy. Also, scanning electron microscopy was an extremely helpful technique for identifying the porous structure of the films, structure that will provide a high surface area. A high surface area of the deposit is wanted because these deposits are meant to be used as supercapacitor plates.”

## 2. Methods of investigation

The X-ray diffraction spectroscopy method was employed in order to characterize the Ni-Cu films from the crystallographic point of view. The analyses were performed on a Bruker D8 ADVANCE X-ray diffractometer equipped with a Cu  $\alpha$  radiation source with a wavelength of 1.54060nm. The analysis parameters were: angle of 0-90°, a voltage of 40kV and a power of 40mA. The X-ray diffraction spectroscopy is a rapid and reproducible instrumental technique used in previous studies [8-10] for the identification of solid components and for the proportion of different component minerals.

The Raman investigations were carried out with a Renishaw InVia micro-Raman spectrometer with a laser source with a wavelength of 532nm and a full power of 500mW. In order to analyze the samples, one has used a 1800l/mm holographic grid, at a 5% power, an exposure time of 20s and 20 acquisition.

The scanning electron microscopy has been used in order to determine the morphology and the structure of the deposition crystals. The analyses were performed on a ZEISS Merlin Gemini II scanning electron microscope with a resolution of 0.9 nm.

## 3. Results and discussions

In order to determine if the electrodeposited Ni-Cu films could be used as potential supercapacitors electrodes, as reported in [11-13], one has used three complementary characterization techniques to reveal the Ni-Cu properties, namely X-ray diffraction spectroscopy, Raman spectroscopy and Scanning electron microscopy (SEM).

The electrochemical cell used for the deposition of the Ni-Cu layers was composed of a steel plate that worked as

a cathode, a platinum mesh that worked as anode, an electrolyte solution composed of 0.5M  $\text{CuSO}_4 \cdot 5\text{H}_2\text{O}$  (Sigma-Aldrich), 0.01M  $\text{NiSO}_4 \cdot 7\text{H}_2\text{O}$  (Sigma-Aldrich), 1.5M  $\text{H}_2\text{SO}_4$  (Chim Reactiv), 1M  $\text{HCl}$  (Chim Reactiv), a variable resistance, a power source and an ammeter. One has used an electrolyte solution of this composition in order to achieve a higher conductivity of the solution due to the sulphuric acid and to achieve the complexation of the Cu and Ni ions due to the chlorine provided by the chlorhidric acid [14-16]. Also, the acidic pH of the solution prevents the formation of cooper and nickel hydroxides.

In order to maintain the deposition temperature constant, one has used a thermostatic water bath. The temperature of the deposition solution was 30°C for all the analyzed samples. After the deposition, one has dried the layers by a thermal treatment performed at 180°C, for one hour.

The deposition parameters used for the obtaining of the Ni-Cu films used as samples for the above mentioned analyses are as follows:

- sample 1: current density of 1.5  $\text{A}/\text{cm}^2$  and a time of deposition of 125 seconds;
- sample 2: current density of 1.1  $\text{A}/\text{cm}^2$  and a time of deposition of 125 seconds;
- sample 3: current density of 0.7  $\text{A}/\text{cm}^2$  and a time of deposition of 125 seconds;
- sample 4: current density of 1.5  $\text{A}/\text{cm}^2$  and a time of deposition of 50 seconds;
- sample 5: current density of 1.1  $\text{A}/\text{cm}^2$  and a time of deposition of 50 seconds;
- sample 6: current density of 0.7  $\text{A}/\text{cm}^2$  and a time of deposition of 50 seconds.

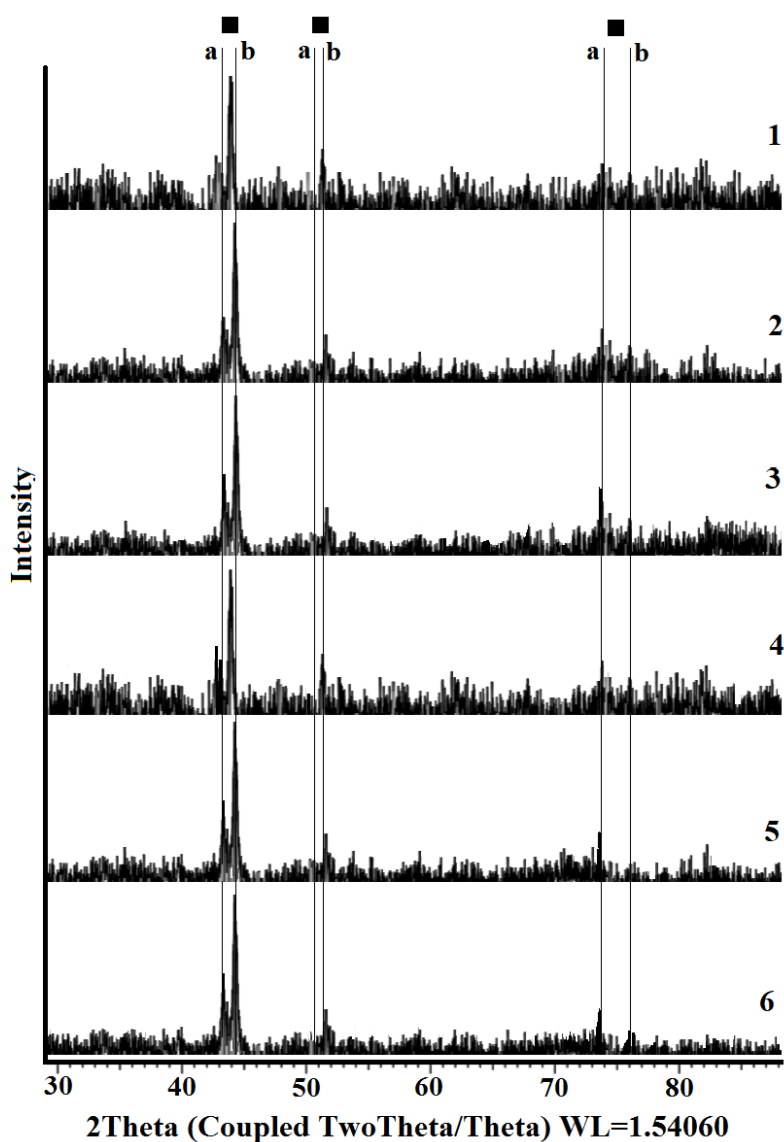


Fig. 1. XRD patterns of the Ni-Cu deposits at different parameters a: metallic Cu, b: metallic Ni, ■: Ni-Cu alloy

### 3.1. Deposition crystallography

In order to have a crystallographic image of the Ni-Cu deposited layers, one has performed a X-ray diffraction spectroscopy analysis. The diffraction patterns were recorded between the angles  $0^\circ$  and  $90^\circ$ . Comparing the obtained data with the data from the literature, it appears that the type of crystallization of the Ni-Cu alloy is a cubic type of FCC [17-21], this is due to the fact that the lattice sizes of Cu and Ni are similar (3.615 and 3.524 Å) [22,23].

Fig. 1 illustrates the XRD patterns of the Ni-Cu layers deposited on steel plates. One may see that the obtained spectrum has three main reflections which belong to the (111), (200) and (220) crystal planes, at angles of  $43.4^\circ$ ,  $50.7^\circ$  and  $74.7^\circ$  specific for a fcc metallic copper, according to International Centre for Diffraction Data (ICDD) file 00-009-0205. According to ICDD file 00-077-7710, for the metallic nickel, the corresponding reflections are at  $44.4^\circ$ ,  $51.8^\circ$  and  $76.3^\circ$  which belong to the (111), (200) and (220) crystal plane, respectively. The reflections obtained at  $43.6^\circ$ ,  $50.8^\circ$  and  $74.6^\circ$ , which belong to the

(111), (200) and (220) crystal plane is assigned to Cu-Ni alloy (ICDD file 00-047-1406) [22, 24-29].

Some nickel and copper oxides may appear due to the thermal treatment applied immediately after the layer deposition. The presence of these oxides is highlighted by the presence of low reflections at angles of  $37.1^\circ$ ,  $43.2^\circ$ ,  $62.7^\circ$  and  $75.2^\circ$ , which are representative for the crystalline planes (111), (200), (222) and (311) respectively for nickel copper oxide according to ICDD 01-078-0646.

### 3.2. Raman analysis

The micro-Raman analysis was performed at room temperature and room atmosphere. The study was performed on Ni-Cu deposition layers in order to detect the presence of Ni and Cu in the deposit and to determine the surface crystalline form.

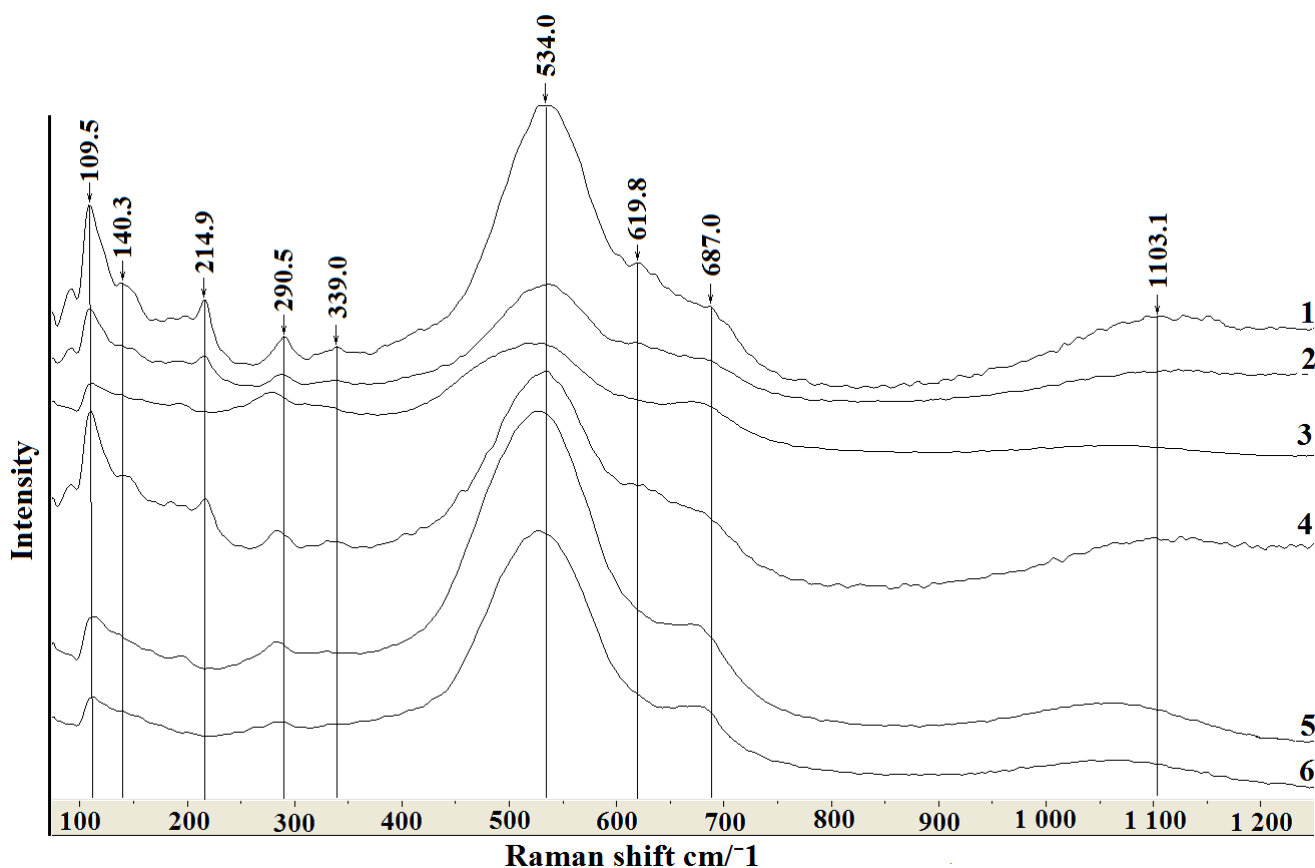


Fig. 2. Raman spectrum of the Ni-Cu deposition

The Raman spectra of the Ni-Cu electrodeposited layers are shown in Figure 2. The Ni-Cu coating is highlighted by the presence of nine characteristic peaks of nickel and copper oxides. The peaks between 109 and 619  $\text{cm}^{-1}$  correspond to copper oxides such as:  $\text{Cu}_2\text{O}$  (109, 140 and 214  $\text{cm}^{-1}$ ) and  $\text{CuO}$  (290, 339 and 619  $\text{cm}^{-1}$ ) [30-32]. One may see the presence of some other peaks at 534 and

1103  $\text{cm}^{-1}$  that could be attributed to the vibration of the NiO bond [30,33,34]. The medium Raman signal observed at 687  $\text{cm}^{-1}$  is assigned to the ring breathing mode [33] respectively for the ring stretch [35, 36].

### 3.3. Crystals dimensions

In the electrodeposition process of the Ni-Cu films, a secondary reaction that takes place is the evolution of hydrogen. The bubbles generated on the surface of the electrode, disturb the continual growth of the crystal thus generating a tree structure, also called dendritic structure [13, 29, 37-38]. The growth of cubic crystals takes place in the direction of the octahedral axes, forming long branches on several axes of crystallization (Figure 3).

In order to determine the size of the crystals, scanning electron microscopy was used. The length of a dendritic structure (the tree structure) varies between 1-2 $\mu$ m and the width varies between 300-800nm. The size of the crystals for the analyzed samples has varied between 70-150nm.

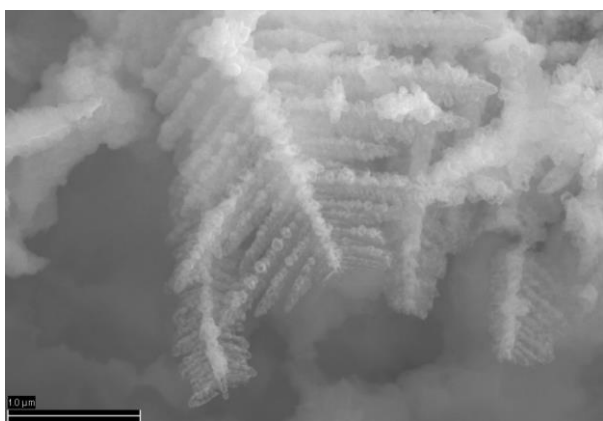


Fig. 3. SEM image of a Ni-Cu deposition

### 4. Conclusions

In this study, some Ni-Cu films electrodeposited on steel plates were analyzed in order to give determine the morphology and crystal structure of these deposits. Regardless of the parameters applied for the deposition process, the morphology and the crystallization system are the same.

XRD results indicated the presence of metallic copper and nickel and also the presence of a nickel-copper alloy with a face centered cubic crystallization system.

Raman spectroscopy results highlighted the presence of the Cu<sub>2</sub>O, CuO and NiO.

Scanning electron microscopy results showed that the growth of cubic crystals takes place direction of the octahedral axes, forming long branches over several crystallization axes, thus obtaining a dendritic structure with dimensions between few nanometers and 1-2 micrometers.

### Acknowledgements

Special thanks go to Mr. Corneliu Andrei for providing the logistic support. Miss Oana Claudia Ciobotea-Barbu is financially supported by the Ministry of

National Education of Romania doctoral grants. The analysis was performed at MICROCOSMOS Laboratory from Geological Institute of Romania.

### References

- [1] M. Alper, H. Kockar, M. Safak, M. C. Baykul **453**, 15 (2008).
- [2] C. E. Dubé, B. Workie, S. P. Kounaves, A. Robbat Jr., M. L. Aksu, *J. Electrochem. Soc.* **142**, 3357, (1995).
- [3] E. Pellicer, A. Varea, S. Pané, K. M. Sivaraman, B. J. Nelson, S. Suriñach, M. D. Baró, J. Sort, *Surf. Coat. Technol.* **205**, 5285 (2011).
- [4] K. Robinson, D. J. Tweet, *Surface X-ray diffraction, Rep. Prog. Phys.* **55**, 599 (1992).
- [5] T. Zafar, B. Bari, K. Alamgir, S. Khalid, M. Arshad, M. N. Anjum, *OAM-RC*, **12**, 337, (2018).
- [6] X. Y. Wang, J. B. Zheng, K. Qiao, J. R. Qu, C. D. Cao, *Appl. Surf. Sci.* **297**, 188 (2014).
- [7] T. Rus, E. Radu, I. Lingvay, M. Lingvay, O. C. Ciobotea-Barbu, C. Campureau, F. M. Benga, G. C. Lazar, D. I. Vaireanu, *U. P. B. Sci. Bull. Series B* **79**, 167 (2017).
- [8] S. Serafima, O. G. Dului, M.-M. Manea, A.-V. Bojar, C. Costea, D. Birgaoanu, O.-C. Barbu, *Rom. Rep. Phys.*, In press, (2018).
- [9] Gh. Nechifor, G. L. Radu, *Tehnici experimentale în analiza Chimică*, Editura Printech, Bucuresti, p. 397 (2004).
- [10] C. Banciu, M. Lungulescu, A. Băra, L. Leonat, A. Teișanu, *OAM-RC.*, **11**, 368, (2017).
- [11] O. C Ciobotea-Barbu, I. A Ciobotaru, F. M. Benga, D. I. Vaireanu, *Rev. Chim. (Bucharest)* **70**(1), 45 (2019).
- [12] O. C Ciobotea-Barbu, I. A Ciobotaru, A. Cojocaru, F. M. Benga, D. I. Vaireanu, *Rev. Chim. (Bucharest)* **70**(7), In press, (2019).
- [13] O. C Ciobotea-Barbu, I. A Ciobotaru, A. Cojocaru, F. M. Benga, D. I. Vaireanu, *Rev. Chim. (Bucharest)*, **70**(8) In press, (2019).
- [14] S. Eugenio, T. M. Silva, M. J. Carmezim, R. G. Duarte, M. F. Montemor, *J. Appl. Electrochem.* **44**, 455 (2014).
- [15] C. Gabrielli, P. Moçotéguy, H. Perrot, R. Wiart, *J. of Electroanal. Chem.* **572**, 367 (2004).
- [16] S. K. Meher, P. Justin, G. Ranga Rao, *Nanoscale* **3**, 683 (2011).
- [17] Zoran Stevic, *New generation of electric vehicles*, Ch. 5, IntechOpen, Serbia, 135 (2012).
- [18] A. R. Naghash, T. H. Etsell, S. Xu, *Chem. Mater.* **18**, 2480 (2006).
- [19] *Știința și Ingineria Materialelor*. <https://gabriel2design.files.wordpress.com/2011/11/sim-curs-6.pdf>, 2011.
- [20] W. P. Davey, *Phys. Rev.* **25**, 755 (1925).
- [21] J. Liu, Y. Zheng, S. Hou, *RSC Adv.* **7**, 37823 (2017).
- [22] Q. Wu, L. D. L. Duchstein, G. L. Chiarello, J. M. Christensen, C. D. Damsgaard, C. F. Elkjær,

- J. B. Wagner, B. Temel, J.-D. Grunwaldt, A. D. Jensen, *Chem. Cat. Chem.* **6**, 301 (2014).
- [23] J.-K. Chang, S.-H. Hsu, I.-W. Sun, W.-T. Tsai, *J. Phys. Chem. C* **112**, 1371 (2008).
- [24] N. Rajasekaran, S. Mohan, *J. Appl. Electrochem* **39**, 1911 (2009).
- [25] R. Mishra, R. Balasubramaniam, *Corros. Sci.* **46**, 3019 (2004).
- [26] L. De L. S. Valladares, A. Ionescu, S. Holmes, C. H. W. Barnes, *J. Vac. Sci. Technol. B* **32**, 051808-1 (2014).
- [27] C.-J. Chen, K.-L. Lin, *J. Electrochem. Soc.* **146**, 137 (1999).
- [28] D. S. Lashmore, M. P. Dariel, *ECS J. Solid State Sci. Technol.* **135**, 1218 (1988).
- [29] B. N. Choi, W. W. Chun, A. Qian, S. J. Lee, C.-H. Chung, *Nanoscale* **7**(44), 18561 (2015).
- [30] S. Chen, L. Brown, M. Levendorf, W. Cai, S.-Y. Ju, J. Edgeworth, X. Li, C. W. Magnuson, A. Velamakanni, R. D. Piner, J. Kang, J. Park, R. S. Ruoff, *ACS Nano* **5**, 1321 (2011).
- [31] G. Niaura, *Electrochim. Acta*, **45**, 3507 (2000).
- [32] M. H. Chou, S. B. Liu, C. Y. Huang, S. Y. Wu, C.-L. Cheng, *Appl. Surf. Sci.*, **254**, 7539 (2008).
- [33] H. C. Garcia, R. Diniz, M. I. Yoshida, L. Fernando C. de Oliveira, *Cryst. Eng. Comm*, **11**, 881 (2009).
- [34] Y. Ishida, Y. Mita, M. Kobayashi, S. Endo, *Phys. Stat. Sol. (b)* **235**, 501 (2003).
- [35] Al. A. Kolomenskii, S. N. Jerebtsov, J. A. Stoker, M. O. Scully, H. A. Schuessler, *J. Appl. Phys.* **102**, 094902 (2007).
- [36] A. A. Kolomenskii, H. A. Schuessler, *Spectrochim. Acta, Part A* **61**, 647, (2005).
- [37] Y. Wang, J. Ghanbaja, F. Soldera, P. Boulet, D. Horwat, F. Mücklich, J.F. Pierson, *Acta Mater.* **76**, 207 (2014).
- [38] S. Cherevko, N. Kulyk, C.-H. Chug, *Nanoscale* **4**, 568 (2012).

---

\*Corresponding author: di\_vaireanu@yahoo.co.uk